

Magnetic and thermal properties of three ionothermally synthesized metal–carboxylate frameworks of $[M_3(ip)_4][EMIm]_2$ ($M = Co, Ni, Mn$, $H_2ip =$ isophthalic acid, $EMIm =$ 1-ethyl-3-methyl imidazolium)[†]

Wen-Xian Chen, Gui-Lin Zhuang, Hai-Xia Zhao, La-Sheng Long,* Rong-Bin Huang and Lan-Sun Zheng

Received 14th January 2011, Accepted 9th May 2011

DOI: 10.1039/c1dt10070j

Three metal–organic frameworks, $[M_3(ip)_4][EMIm]_2$ ($M = Co$ **1**, Ni **2**, Mn **3**, $H_2ip =$ isophthalic acid, $EMIm =$ 1-ethyl-3-methyl imidazolium) were prepared from an ionic liquid medium. All the compounds feature the same $(4^{2+})(6^4)$ topology based on linear trinuclear clusters as eight-connected nodes. Compounds **1** and **2** are isostructural, while compound **3** exhibits a different structure due to the slight difference in the arrangement of $M_3(OOCR)_8$ SBUs. Magnetic property measurements reveal that all the compounds display anti-ferromagnetic coupling, where compounds **2** and **3** show isotropic exchange interactions of -0.10 cm^{-1} for **2** and -1.6 cm^{-1} for **3**. Investigation of the thermal diffusivity shows that the thermal diffusivity of **1** is higher than that of **3**, while that of **3** is higher than that of **2**.

Introduction

Significant efforts have been expended towards construction of various functional coordination materials through traditional hydro/solvothermal reactions, resulting in important developments in the past years.^{1,2} However, developing novel solid-state polymeric architectures through new synthetic strategies is still a challenge. Ionothermal synthesis as a promising synthetic technique especially for the preparation of zeotypes³ and coordination polymers⁴ is of particular interest. Firstly, the peculiar physicochemical properties of ionic liquids (ILs) such as low melting points, high thermal stability and negligible vapor pressure,⁵ allows ionothermal synthesis to be more environmentally-friendly and safer than hydro/solvothermal reactions. Moreover, the cations of the ionic liquid not only act in a charge-compensating and space-filling role in the materials, but also direct the formation of different structural patterns from those obtained using a routine synthetic approach, despite the same organic ligand being employed.⁶ Finally, tuning the solvent properties by combining the cations and the anions in various ways, could be an approach to design the structures of coordination polymers.⁷ With these properties, ionothermal synthesis has experienced a drastic development in the past several years.⁸ Although extensive research efforts have been devoted to studying the influence of the cation or the anion,

or the cation and anion of the ILs on the structures of ionothermal materials, the effect of metal centers in ionothermal reactions remains largely unexplored. On the other hand, although ILs are known to possess a high thermal capacity, investigation of the thermal diffusivity of ionothermally synthesized metal–organic frameworks has never been performed.

Utilizing the derivative of isophthalic acid as the supporting ligand, we have reported the syntheses of 4f and 3d–4f heterometallic frameworks under ionothermal conditions.⁹ As an expansion of our study, we report herein three ionothermally synthesized materials $[M_3(ip)_4][EMIm]_2$ ($M = Co$ **1**, Ni **2**, Mn **3**, $H_2ip =$ isophthalic acid) generated under the same reaction conditions. Crystal structural analysis reveals that all the three compounds feature $(4^{2+})(6^4)$ topology based on the $M_3(OOCR)_8$ clusters as eight-connected nodes. Magnetic property measurements indicate that all compounds display anti-ferromagnetic coupling. Investigation of the thermal diffusivity shows that the thermal diffusivity of **1** is higher than that of **3**, while that of **3** is higher than that of **2**.

Experimental**Materials and physical measurements**

All the reagents and solvents employed were commercially available and used as received without further purification. The C, H, and N microanalyses were carried out with a CE instruments EA 1110 elemental analyzer. The FT-IR spectra were recorded in the range of $4000\text{--}400\text{ cm}^{-1}$ with a Nicolet AVATAR FT-IR360 spectrometer. The X-ray powder diffractometry (XRPD) study was performed on Panalytical X-Pert pro diffractometer with $Cu\text{-K}\alpha$ radiation. The thermogravimetric analysis (TGA) was performed with a NETZSCH STA 449C instrument. Thermal diffusivity was measured by NETZSCH LFA 457 NanoFlash.

State Key Laboratory of Physical Chemistry of Solid Surface and Department of Chemistry, College of Chemistry and Chemical Engineering, Xiamen University, Xiamen, 361005, China. E-mail: lslong@xmu.edu.cn; Fax: +86 592 218 3047

[†] Electronic supplementary information (ESI) available: X-ray crystallographic files in cif format for complexes **1–3**, program XMMAG and X-ray powder diffraction for the residual products of **1** to **3**. CCDC reference numbers 809087–809089. For ESI and crystallographic data in CIF or other electronic format see DOI: 10.1039/c1dt10070j

Table 1 Crystal data and details of the data collection and refinement for compounds **1** to **3**

Complex	1	2	3
Formula	C ₄₄ H ₃₈ N ₄ O ₁₆ Co ₃	C ₄₄ H ₃₈ N ₄ O ₁₆ Ni ₃	C ₄₄ H ₃₈ N ₄ O ₁₆ Mn ₃
<i>M_r</i>	1055.57	1054.91	1043.6
Crystal system	Orthorhombic	Orthorhombic	Monoclinic
Space group	<i>Pbca</i>	<i>Pbca</i>	<i>P2₁/c</i>
<i>a</i> /Å	15.414(3)	15.491(2)	13.092(3)
<i>b</i> /Å	11.877(2)	11.669(3)	14.490(3)
<i>c</i> /Å	24.154(5)	23.750(2)	12.640(3)
α (°)	90	90	90
β (°)	90	90	116.85(3)
γ (°)	90	90	90
<i>V</i> /Å ³	4421.7(15)	4293.1(3)	2139.3(7)
<i>Z</i>	4	4	2
<i>D_c</i> /g cm ⁻³	1.586	1.632	1.620
μ /mm ⁻¹	1.190	1.382	0.952
No. of data/parameter	4335/306	4206/350	4195/304
θ range/°	3.14–26.00	2.78–26.00	3.23–26.00
Obs reflns	2418	2569	2903
<i>R</i> ₁ [<i>I</i> > 2 σ (<i>I</i>)]	0.0637	0.0389	0.0579
<i>wR</i> ₂ (all data)	0.1758	0.0702	0.1795

$$R_1 = \frac{\sum \|F_o\| - |F_c|}{\sum |F_o|}, wR_2 = \left[\frac{\sum w(F_o^2 - F_c^2)^2}{\sum w(F_o^2)^2} \right]^{1/2}.$$

Magnetic susceptibility was measured by a Quantum Design MPMS superconducting quantum interference device (SQUID).

X-Ray crystallography

Data collections were performed on a Rigaku R-AXIS RAPID IP diffractometer at 293 K for **1**, 173 K for **3** and on an Oxford Gemini S Ultra CCD area detector at 173 K for **2**. Absorption corrections were applied by using the analytical program Tompa-analytical for **1**, **3** and multiscan program CrysAlis Red for **2**. The structures were solved by direct methods, and non-hydrogen atoms were refined anisotropically by least-squares on *F*² using the SHELXTL program.¹⁰ The hydrogen atoms of organic ligands were generated geometrically (C–H, 0.96 Å; N–H, 0.90 Å). Crystal data as well as details of data collection and refinement for the compounds are summarized in Table 1. CCDC number of 809087 to 809089 for **1** to **3**.

Synthesis

Compound **1** was ionothermally synthesized as follows: a mixture of 0.249 g Co(OOCCH₃)₂·4H₂O, 0.166 g isophthalic acid and 1.2 g ionic liquid 1-ethyl-3-methyl imidazolium bromide was sealed to a 25 mL Teflon-lined Parr at 140 °C for about a week and then cooled to room temperature at the rate of 3 °C h⁻¹. The dark-purple crystals were obtained in 39.2% yield (based on isophthalic acid). Anal. calcd (found) for Co₃C₄₄H₃₈O₁₆N₄ (%): C, 50.02(49.71); N, 5.31(5.28); H, 3.60(3.64). IR Spectra for **1** (KBr, cm⁻¹): 1607.4 s, 1383 s, 749.3 s, 714.2 s, 1579.4 m, 1480.6 m, 1171.3 m, 448.2 m, 3149.9 w, 3119.3 w, 3082 w, 1264.5 w, 1073.7 w, 824.3 w.

Compound **2** was prepared under similar ionothermal conditions as described for **1**, except that Ni(OOCCH₃)₂·4H₂O was used. Green crystals were obtained in about 40.7% yield (based on isophthalic acid). Anal. calcd (found) for Ni₃C₄₄H₃₈O₁₆N₄ (%): C, 50.05(49.49); N, 5.31(5.46); H, 3.60(3.27). IR Spectra for **2** (KBr, cm⁻¹): 1619.7 s, 1549.1 s, 1379.1 s, 751.3 s, 717.6 s, 1401.2 m, 1169.7 m, 828.6 m, 446.3 m, 3146.6 w, 3119.7 w, 3075.8 w, 1266.4 w, 1073.6 w, 657.1 w.

Compound **3** was prepared under similar ionothermal conditions as illustrated for **1**, except that Mn(OOCCH₃)₂·4H₂O was used. Colorless crystals were obtained in about 37.6% yield (based on isophthalic acid). Anal. calcd (found) for Mn₃C₄₄H₃₈O₁₆N₄ (%): C, 50.60(50.54); N, 5.37(5.28); H, 3.64(3.61). IR Spectra for **3** (KBr, cm⁻¹): 1614.2 s, 1576.1 s, 1383.3 s, 752 s, 712.7 s, 1478.8 m, 1430.0 m, 1172.1 m, 822.1 m, 437.4 m, 3430.4 w, 3115.4 w, 1265 w, 1072.9 w, 655.5 w.

Results and discussion

Compound **1** crystallized in the orthorhombic space group *Pbca*. Crystal structure analysis reveals that the asymmetric unit consists of one and half Co(II) ions, two ip ligands, and one EMIm ion. The coordination environment of the Co(II) ions is best described as a distorted octahedron. Co1 is six coordinated by six monodentate carboxylates, respectively from six ip ligands. Co2 is coordinated by two chelate carboxylates and two monodentate carboxylates, respectively from four ip ligands. The Co–O distances range from 1.991(4) to 2.386(4) Å, comparable to those in the reported Co-complex.¹¹ Each independent Co1 center bridged two adjacent Co2 ions *via* two carboxylate groups in a *syn–syn* fashion and one carboxylate group in chelating/bridging mode generates a trinuclear unit M₃(OOCR)₈ as shown in Fig. 1c. The Co···Co distance separated by the carboxylate group is 3.528 Å. Such a trinuclear unit is further linked to eight neighboring trinuclear units through eight ip ligands, leading to a three-dimensional open framework. The EMIm cations of the ionic liquid, acting as charge-compensating agents, are located in the voids of the anionic framework. The overall structure of the 3D network can be described as a 8-connected net linked by M₃(OOCR)₈ SBUs as 8-connected nodes (Fig. 1e). The 8-connected net in **1** shown in Fig. 1f can be further specified by the Schläfli symbol (4²⁴)(6⁴) where the shortest rings meeting at the twenty four and four angles of the 8-connected vertices, are 4- and 6-membered rings respectively. Compound **2** is isostructural to **1**. The bond lengths of Ni–O are 1.962(2)–2.239(2) Å, comparable to those in the reported Ni-complex.¹² The Ni···Ni distance is 3.444 Å.

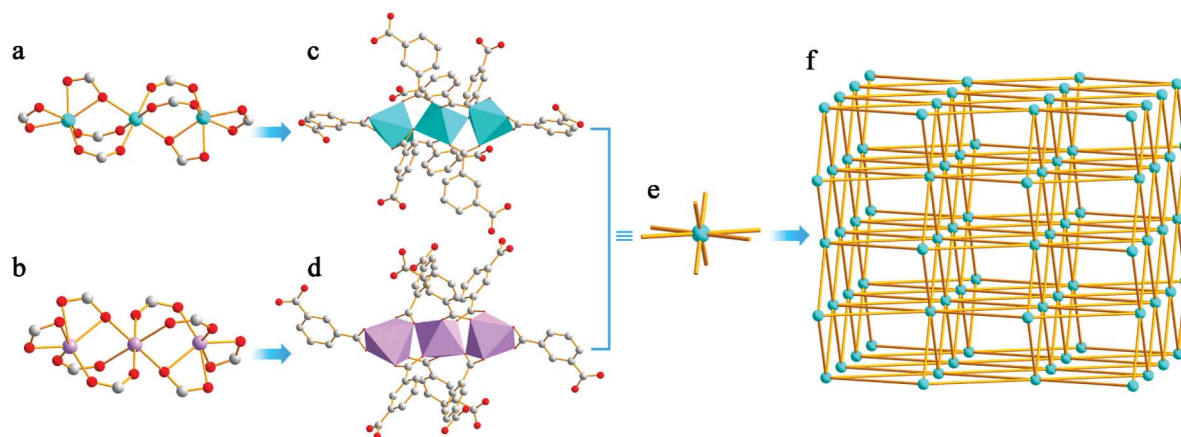


Fig. 1 Coordination environments of the trinuclear cluster in **1** and **2** (a), and **3** (b); Two different trinuclear structures in **1** and **2** (c), and **3** (d); A schematic view of the connections of one node (e); The 4^{246^4} topological network of **1**–**3** (f).

Different from **1** and **2**, compound **3** crystallized in the monoclinic space group $P2_1/c$. Crystal structure analysis reveals that **3** has the same topology as that of **1** and also exhibits a 3D anionic framework consisting of trinuclear units $M_3(\text{OOCR})_8$ (Fig. 1d) as 8-connected nodes (Fig. 1e). However, the arrangement of $M_3(\text{OOCR})_8$ SBU in **3** is significantly different from these in **1** and **2** (Fig. 2), which is attributed to the radius of the manganese ion being larger than those of the cobalt and nickel ions, and because repulsion between ip ligands and EMIm ions in the anionic framework would be greatly increased if the arrangement of the

$M_3(\text{OOCR})_8$ SBU in **1** and **2** adopted a similar arrangement with that in **3**. Consistently, although the same organic ligand was employed,¹³ and even the same topology was adopted,¹⁴ the structures of **1** and **2** are very different from that of the Co(II)-based framework obtained from solvothermal reactions, while the structure of **3** is similar to that of the Co(II)-based framework obtained from solvothermal reactions, due to the fact that the $\text{H}_2\text{N}(\text{CH}_3)_2^+$ in the Co(II)-based framework is significantly smaller than the EMIm ions in present work. It was mentioned that, although the solvent-accessible volumes and pore volume ratios of three compounds calculated through the PLATON program¹⁵ are 1653.9 \AA^3 (37.4%) for **1**, 1584.0 \AA^3 (36.9%) for **2** and 717.6 \AA^3 (33.5%) for **3**, respectively, utilization of the anionic frameworks to perform cation exchange was a failure, due to the pore window being too small to allow the EMIm ions to be removed from the pores.

Magnetic properties of **1**–**3** were investigated through variable-temperature susceptibility measurements in the temperature range from 2.0 to 300 K with an applied magnetic field of 1000 Oe. For **1**, the $\chi_M T$ value at room temperature is $9.45 \text{ cm}^3 \text{ mol}^{-1} \text{ K}$, which is considerably larger than the spin-only value of $5.63 \text{ cm}^3 \text{ mol}^{-1} \text{ K}$ calculated for three high-spin Co(II) ions ($S = 3/2$, $g = 2$) due to the orbital contribution from single Co(II) ions (Fig. 3a). Upon lowering the temperature, the $\chi_M T$ value continuously decreases to a minimum value of $6.50 \text{ cm}^3 \text{ mol}^{-1} \text{ K}$ (5 K), indicating dominant intramolecular antiferromagnetic interactions. Compound **1** behaves as a Curie–Weiss paramagnet above 100 K, which can be fitted with a Weiss constant of -11.15 K and a Curie constant of $9.83 \text{ cm}^3 \text{ mol}^{-1} \text{ K}$.¹⁶ Attempts to simulate the magnetic susceptibility by spin-Hamiltonian with the help of our program *XMMAG* (Supporting information S1†) failed, because six-coordinate Co(II) ions present considerable first-order orbital momentum, and the spin-Hamiltonian must be supplemented by the orbital-dependent exchange interactions and spin–orbit coupling effects.¹⁷ It should be mentioned here that the coordination polymer $[\text{H}_2\text{N}(\text{CH}_3)_2]_2[\text{Co}_3(\text{ip})_4] \cdot \text{H}_2\text{O}$ previously reported by Zheng *et al.*,¹⁴ which features the same topology of the 3D network and bridging mode of the trinuclear unit as that of **1**, displays ferromagnetic interactions. Scrutinizing their structure reveals that the Co...Co distance (3.528 \AA) and

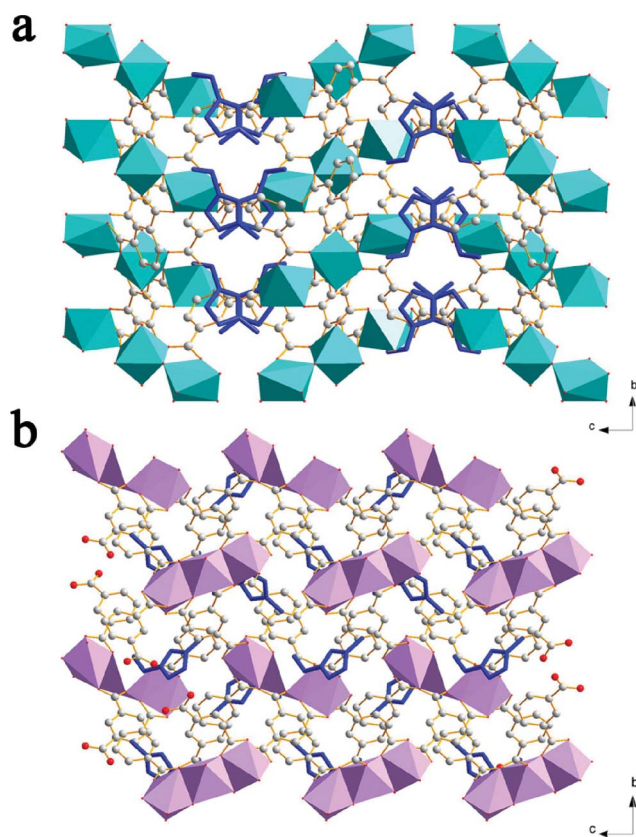


Fig. 2 3D network of **1** and **2** (a), and **3** (b) along the a axis.

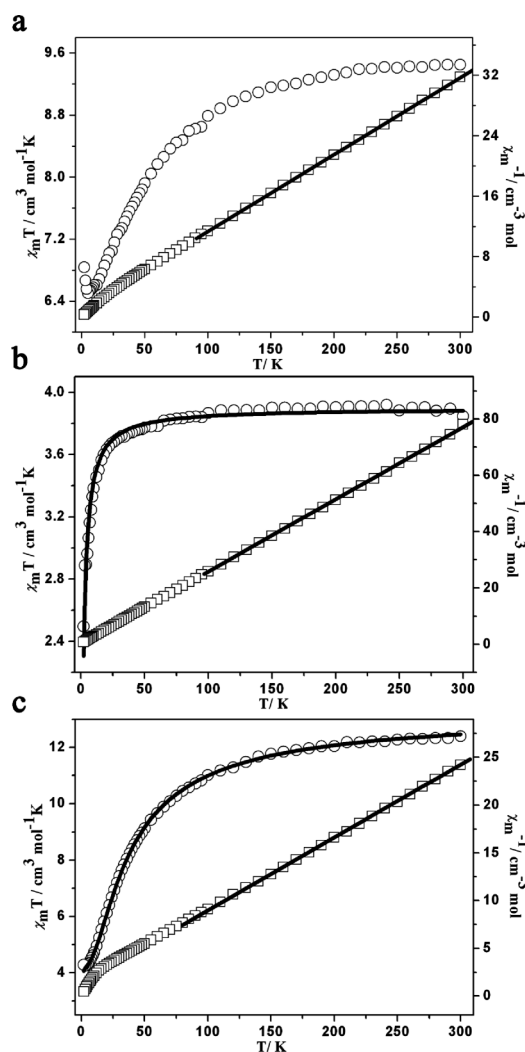


Fig. 3 Plot of $\chi_M T$ vs. T (denoted o) and χ_M^{-1} vs T (denoted \square) for **1** (a), **2** (b), **3** (c).

Co–O–Co angle (108.08°) in the unit of **1** are very close to those (3.533 \AA , 108.47°) in $[\text{H}_2\text{N}(\text{CH}_3)_2][\text{Co}_3(\text{ip})_4]\cdot\text{H}_2\text{O}$, implying that the magnetic difference may be attributed to the presence of different guest molecules.¹⁸

For **2** and **3**, the resulting $\chi_M T$ vs. T plot is given in Fig. 3b and Fig. 3c respectively. The $\chi_M T$ value at room temperature (300 K) is $3.85 \text{ cm}^3 \text{ mol}^{-1} \text{ K}$ for **2** and $12.39 \text{ cm}^3 \text{ mol}^{-1} \text{ K}$ for **3**, consistent with the value expected for three independent metal ions in the molecule, following a Curie law¹⁶ with (Ni^{2+} , $g = 2.26$ for **2**; Mn^{2+} , $g = 1.95$ for **3**). As the temperature decreases, the value of $\chi_M T$ for **3** decreases slowly and reaches the minimum $4.37 \text{ cm}^3 \text{ mol}^{-1} \text{ K}$ at 2 K, while for **2** it does not decrease slowly until 18 K and then decreases abruptly and reaches the minimum $2.49 \text{ cm}^3 \text{ mol}^{-1} \text{ K}$ at 2 K. Furthermore, the linear fit was performed for χ_M^{-1} vs. T following the Curie–Weiss law,¹⁶ $\chi_M = C/(T - \theta)$, which gives a set of parameters: $C = 3.90 \text{ cm}^3 \text{ mol}^{-1} \text{ K}$, $\theta = -0.81 \text{ K}$ for **2** and $C = 13.10 \text{ cm}^3 \text{ mol}^{-1} \text{ K}$, $\theta = -17.63 \text{ K}$ for **3**. These results indicate that **2** and **3** in general exhibit antiferromagnetic coupling between two metal ions through $\mu^2\text{:}\eta^1\text{:}\eta^2\text{-}$ carboxylate bridges.

In order to elucidate the magnetic exchange interactions in **2** and **3**, the magnetic susceptibilities were fitted with the help of our

program *XMMAG* in which isotropic exchange interactions (J) and inter-unit interaction (zJ) were taken into account. The best fit gives a set of parameters: $J = -0.10 \text{ cm}^{-1}$, $g = 2.28$, $zJ = -0.19 \text{ cm}^{-1}$ and $R = 2.0 \times 10^{-4}$ for **2**; $J = -1.60 \text{ cm}^{-1}$, $g = 2.00$, $zJ = -0.02 \text{ cm}^{-1}$ and $R = 3.0 \times 10^{-5}$ for **3**, where R is calculated from $\sum[(\chi_M T)_{\text{obs}} - (\chi_M T)_{\text{calcd}}]^2 / \sum[(\chi_M T)_{\text{obs}}]^2$. The negative J value exclusively reveals low antiferromagnetic exchange between metal ions. The negative zJ value also indicates antiferromagnetic exchange between the adjacent units.

Thermogravimetric analysis (TGA) studies were performed in an air atmosphere at a heating rate of $10 \text{ }^\circ\text{C min}^{-1}$ for **1–3**. As shown in Fig. 5, the TGA diagrams of **1–3** display no weight loss before the temperature of $360 \text{ }^\circ\text{C}$ for **1**, $380 \text{ }^\circ\text{C}$ for **2** and $350 \text{ }^\circ\text{C}$ for **3**. As the temperature further increases, **1–3** rapidly decompose and the weight loss is steep until the temperature reaches $473 \text{ }^\circ\text{C}$ for **1**, $456 \text{ }^\circ\text{C}$ for **2** and $476 \text{ }^\circ\text{C}$ for **3**, indicating the removal of counter ions and organic ligands. The residual weight of 22.5%, 21.7% and 21.8% respectively for **1** to **3** is consistent with the calculated values of 22.8% for Co_3O_4 in **1**, 21.2% for NiO in **2** and 22.7% for Mn_2O_3 in **3** respectively. The residual products were proved by X-ray powder diffraction (Supporting information, Fig. S1 to S3[†]).

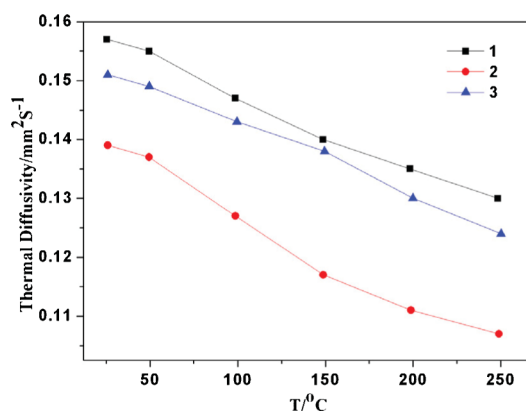


Fig. 4 Thermal diffusivity for **1–3**.

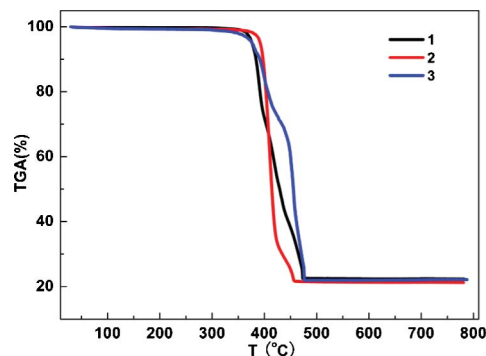


Fig. 5 TG curves from room temperature to $800 \text{ }^\circ\text{C}$ for **1–3**.

Owing to ILs possessing high thermal capacity, it is expected that compounds **1** to **3** have lower thermal diffusivity and function as new heat-resistant materials. Accordingly, the Flash Method was used to perform thermal diffusivity measurements of **1** to **3** on the basis of their pellet samples. The resulting thermal diffusivity of **1** to **3** at different temperatures are shown in Fig. 4. The

thermal diffusivity values at room temperature are 0.157, 0.139 and 0.151 mm² S⁻¹ K for **1** to **3** respectively and decrease with the increase of temperature. Such low thermal diffusivity values are close to that of plastic, indicating that ionothermally synthesized compounds may be good candidates for heat-resistant materials. Since **1** and **2** are isostructural, the observed thermal diffusivity of **1** which is higher than that of **2** indicates that it is the density of the framework that plays a key contribution to their thermal diffusivity, and the higher the density of the framework, the lower the thermal diffusivity. This result is different from that reported by J. M. Devi and coworkers, in which the thermal diffusivity of the complexes increases with the decrease in the mass and increase in the free electron density of the metal ion coordinated.¹⁹ It was mentioned that, although the density of **3** is close to that of **2**, and significantly larger than that of **1**, the thermal diffusivity of **3** is close to that of **1**, instead of close to that of **2**, which may be due to the fact that the structure of **3** is different from those of **1** and **2**.

Conclusions

In summary, three metal-organic frameworks based on linear trinuclear clusters as 8-connected nodes were prepared under ionothermal conditions. All the compounds feature the same a (4²⁴)(6⁴) topology. Their structures are significantly different from those obtained from hydrothermal or solvothermal reactions, indicating that ionic liquids serve as the cationic structure-directing agent in the formation of the host networks. Magnetic property measurement reveals that all compounds display anti-ferromagnetic coupling, while the thermal diffusivity study shows that their thermal diffusivity is in the order of **1** > **3** > **2**.

We thank the NNSFC (Grant Nos. 20825103, 90922031 and 21021061), the 973 project (Grant 2007CB815304) from MSTC for the financial support.

References

- (a) L. Pan, B. Parker, X. Huang, D. H. Olson, J. Y. Lee and J. Li, *J. Am. Chem. Soc.*, 2006, **128**, 4180; (b) X.-J. Kong, Y.-P. Ren, P.-Q. Zheng, Y.-X. Long, L.-S. Long, R.-B. Huang and L.-S. Zheng, *Inorg. Chem.*, 2006, **45**, 10702; (c) X.-J. Kong, Y.-P. Ren, W.-X. Chen, L.-S. Long, Z. Zheng, R.-B. Huang and L.-S. Zheng, *Angew. Chem., Int. Ed.*, 2008, **47**, 2398.
- (a) E. Tang, Y.-M. Dai, J. Zhang, Z.-J. Li, Y.-G. Yao, J. Zhang and X.-D. Huang, *Inorg. Chem.*, 2006, **45**, 6276; (b) M. P. Suh, Y. E. Cheon and E. Y. Lee, *Chem.–Eur. J.*, 2007, **13**, 4208; (c) W.-X. Chen, S.-T. Wu, L.-S. Long, R.-B. Huang and L.-S. Zheng, *Cryst. Growth Des.*, 2007, **7**, 1171.
- (a) E. R. Cooper, C. D. Andrews, P. S. Wheatley, P. B. Webb, P. Wormald and R. E. Morris, *Nature*, 2004, **430**, 1012; (b) E. R. Parnham, P. S. Wheatley and R. E. Morris, *Chem. Commun.*, 2006, 380; (c) E. R. Parnham and R. E. Morris, *J. Am. Chem. Soc.*, 2006, **128**, 2204; (d) E. R. Parnham and R. E. Morris, *Chem. Mater.*, 2006, **18**, 4882; (e) E. A. Drylie, D. S. Wragg, E. R. Parnham, P. S. Wheatley, A. M. Z. Slawin, J. E. Warren and R. E. Morris, *Angew. Chem., Int. Ed.*, 2007, **46**, 7839.
- (a) K. Jin, X. Huang, L. Pang, J. Li, A. Appel and S. Wherland, *Chem. Commun.*, 2004, 2872; (b) D. N. Dybtsev, H. Chun and K. Kim, *Chem. Commun.*, 2004, 1594; (c) Z. Lin, D. S. Wragg and R. E. Morris, *Chem. Commun.*, 2006, 2021; (d) S. Chen, J. Zhang and X. Bu, *Inorg. Chem.*, 2008, **47**, 5567.
- (a) J. G. Huddleston, A. E. Visser, W. M. Reichert, H. D. Willauer, G. A. Broker and R. D. Rogers, *Green Chem.*, 2001, **3**, 156; (b) R. D. Rogers and K. R. Seddon, *Science*, 2003, **302**, 792; (c) K. E. Gutowski, G. A. Broker, H. D. Willauer, J. G. Huddleston, R. P. Swatloski, J. D. Holbrey and R. D. Rogers, *J. Am. Chem. Soc.*, 2003, **125**, 6632; (d) R. Ludwig and U. Kragl, *Angew. Chem., Int. Ed.*, 2007, **46**, 6582.
- (a) L. Xu, E. Y. Choi and Y. U. Kwon, *Inorg. Chem.*, 2007, **46**, 10670.
- (a) Z. Lin, D. S. Wragg, J. E. Warren and R. E. Morris, *J. Am. Chem. Soc.*, 2007, **129**, 10334; (b) Z. Lin, A. M. Z. Slawin and R. E. Morris, *J. Am. Chem. Soc.*, 2007, **129**, 4880; (c) L. Xu, E. Y. Choi and Y. U. Kwon, *Inorg. Chem.*, 2008, **47**, 1907; (d) L. Xu, S. Yan, E. Y. Choi, J. Y. Lee and Y. U. Kwon, *Chem. Commun.*, 2009, 3431.
- (a) E. R. Parnham and R. E. Morris, *Acc. Chem. Res.*, 2007, **40**, 1005; (b) R. E. Morris, *Chem. Commun.*, 2009, 2990.
- W.-X. Chen, Y.-P. Ren, L.-S. Long, R.-B. Huang and L.-S. Zheng, *CrystEngComm*, 2009, **11**, 1522.
- SHELXTL 6.10*, Bruker Analytical Instrumentation, Madison, WI, 2000.
- B. Kersting, *Angew. Chem., Int. Ed.*, 2001, **40**, 3987.
- H. Adams, S. Clunas, D. E. Fenton and D. N. Towers, *J. Chem. Soc., Dalton Trans.*, 2002, 3933.
- F. Luo, J.-M. Zheng and G. J. Long, *Cryst. Growth Des.*, 2009, **9**, 1271.
- F. Luo, Y.-X. Che and J.-M. Zheng, *Cryst. Growth Des.*, 2009, **9**, 1066.
- A. L. Spek, *Acta Crystallogr., Sect. A*, 1990, **46**, C34.
- O. Kahn, *Molecular Magnetism*, VCH, New York, 1993.
- (a) J. M. Herrera, A. Bleuzen, Y. Dromzée, M. Julve, F. Lloret and M. Verdager, *Inorg. Chem.*, 2003, **42**, 7052; (b) D. Maspoch, N. Domingo, D. Ruiz-Molina, K. Wurst, J. M. Hernández, G. Vaughan, C. Rovira, F. Lloret, J. Tejada and J. Veciana, *Chem. Commun.*, 2005, 5035.
- X.-N. Cheng, W.-X. Zhang, Y.-Y. Lin, Y.-Z. Zheng and X.-M. Chen, *Adv. Mater.*, 2007, **19**, 1494.
- J. M. Devi, P. Tharmaraj, S. K. Ramakrishnan and K. Ramachandran, *Mater. Lett.*, 2008, **62**, 852.